Plasma losses by charged particles in thin films: Effects of spatial dispersion, phonons, and magnetic field

Godfrey Gumbs
Department of Physics, University of Lethbridge, Lethbridge, Alberta, Canada T1K 3M4

Norman J. M. Horing
Department of Physics and Engineering Physics, Stevens Institute of Technology, Hoboken, New Jersey 07030

(Received 13 June 1990)

The energy loss of a charged particle to a solid-state plasma film or slab of finite thickness is treated here, both for motion parallel to the slab faces as well as for penetration across the slab. In this, we extend the early work of Ritchie to include nonlocal dispersive plasma features, in addition to the dynamic response features associated with the excitation of slab collective modes. We employ the diagonal approximation for the slab random-phase-approximation inverse dielectric response function, and the plasma electrons are subject to the specular-reflection boundary condition at the slab faces. For parallel motion within the slab, we find modifications to the result of Núñez, Echenique, and Ritchie due to the finite width of the slab. For particle penetration across the slab, we incorporate the dynamic plasma response features associated with phonon polarization and a magnetic field to determine the role of bulk and surface magnetopolaritons in energy loss. Our detailed field-free calculations clearly demonstrate energy-loss contributions associated with the excitation of symmetric and antisymmetric slab surface polaritons as well as bulk polaritons, with computations carried out in full for GaAs.

I. INTRODUCTION

Electron-energy-loss spectroscopy (EELS) has been an important probe of the fundamental dielectric response properties of a solid-state plasma film or slab. This was brought into clear focus by Ritchie's[1] landmark work on the loss of a fast charged particle penetrating across a bounded quantum plasma of finite thickness. In this paper, we extend Ritchie's analysis to treat energy-loss spectroscopy for charged-particle penetration across a nonlocal plasma exhibiting spatial dispersion in a plane-bounded film or slab of finite thickness. In conjunction with this, we incorporate the role of dynamic phonon-magnetoplasmon coupling in the random-phase-approximation (RPA) dielectric response function of the system. Such phonon polarization effects are of interest for semiconductor heterostructures, even at low temperatures and they will be examined in detail here. Our formulation includes a magnetic field (perpendicular to the planar bounding surfaces of the quantum plasma) to facilitate later analysis of it as a richly revealing probe of the properties of matter in this energy-loss context, as it has been historically. Earlier work on nonlocal energy loss has generally been focused on charged particles in transit outside the film or slab, excluding penetration, most often treating the film in a semi-infinite limit.[1-8] Recent work of Streight and Mills[2] also touches upon aspects of plasma nonlocality in EELS in the null magnetic field limit, in the absence of phonon couplings, but with self-consistent wave functions for n-type GaAs with depletion or accumulation layers induced by suitable charge sheets on the finite film surface. In our treatment of the surfaces, we assume the infinite barrier boundary condition for specular reflection of the Fermi sea of electrons within the finite slab. Furthermore, we assume that the trajectory velocity of the incident particle of charge Ze is not modified by its interaction with the medium, i.e., we neglect all recoil effects.

Hayes and co-workers[9,10] and Bending *et al.*[11] have carried out experiments using injected hot-electron spectroscopy in GaAs to demonstrate nonequilibrium carrier transport across thin semiconductor layers. The energies of the charge carriers injected across the semiconductor were significantly in excess of the Fermi energy. The related calculations of Ref. 10 were done neglecting the contributions associated with the surface since the quantity $\omega_p L/v$ was large for the conditions under which the experiments were performed. (Here, ω_p is the bulk plasma frequency, L is the thickness of the slab, and v is the uniform velocity of the injected electrons.) Our work addresses such surface contributions for smaller slabs, whose finite thickness must be considered along with plasma nonlocality and phonon effects in carrier transport across such slabs.

The energy loss of energetic charged particles moving *parallel* to the surface of a *semi-infinite* plasma has been calculated by several authors[12,13] who have taken the frequency and wave-vector dependence of the dielectric function into account. Their calculations were carried out using the specular reflection model of Ritchie and Marusak[14] in which the induced scalar electric potential can be divided into three parts, (i) the potential due to the external charge, (ii) the potential due to its image, and (iii) a fictitious surface charge fixed by the boundary con-

ditions.[15] Our paper includes treatment of the "*parallel*" case in providing the nontrivial extension of this procedure to a nonlocal slab of finite thickness. Our general formulation of dynamic nonlocal plasma-slab energy loss for charged particles is presented in Sec. II. In Sec. III we report the results of our calculations for energy loss of charged particles moving parallel to the finite plasma slab faces both inside and outside. Section IV is devoted to the determination of the energy loss of a charged particle moving perpendicular to the planar surfaces across the dielectric slab. In Sec. V we study the low-velocity limit of energy losses: In this limit, the nonlocal nature of dielectric response is important. Finally, in Sec. VI, our emphasis is on bringing forth jointly the roles of finite slab width, phonon polarization, and the magnetic field in fast particle energy loss in penetrating across a plasma slab.

II. DIELECTRIC RESPONSE FORMULATION OF ENERGY LOSS TO A PLASMA SLAB

We address the problem of energy loss in terms of the effective potential $V(1)$ at space-time point $1=(\mathbf{r}_1,t_1)$ induced by a passing charged particle which impresses the Coulomb potential $U(2)=Ze/|\mathbf{r}_2-\mathbf{R}(t_2)|$ at space-time point $2=(\mathbf{r}_2,t_2)$. It is assumed that the frictional energy loss is small, so the passing particle moves with approximately uniform velocity such that $\mathbf{R}(t_2)=\mathbf{v}t_2+\mathbf{R}_0$. The plasmalike medium responsible for frictional energy loss is characterized by an inverse dielectric function $K(1,2)$, which provides the linear response relation $V(1)=\int d^4 2\, K(1,2)U(2)$, with effective electric field $\mathbf{E}=-\nabla_1 V(1)$ and corresponding perturbed plasma density

$$\rho(1)=-(4\pi e)^{-1}\int d^4 3\,\nabla_1^2[K(1,3)-\delta^4(1,3)]U(3)\ . \tag{1}$$

The frictional force on the passing particle is

$$\mathbf{f}=e\int d^3 1\,\rho(1)\nabla_1 V(1)$$
$$=-\frac{1}{4\pi}\int d^3 1\,\nabla_1^2[V(1)-U(1)]\nabla_1 V(1)\ . \tag{2}$$

It is worth noting that part of this force, the *self-force*, is eliminated through the introduction of the electric field stress tensor since ($\mathbf{E}=-\nabla V, \nabla\times\mathbf{E}=0$)

$$[\mathbf{E}(\nabla\cdot\mathbf{E})-\mathbf{E}\times(\nabla\times\mathbf{E})]_\alpha=\sum_\beta\frac{\partial}{\partial x_\beta}(E_\alpha E_\beta-\tfrac{1}{2}\delta_{\alpha\beta}E^2) \tag{3}$$

and the tensor divergence on the right-hand side of Eq. (3) integrates to zero over all space for a medium of arbitrary inhomogeneity. This yields

$$\mathbf{f}=\frac{1}{4\pi}\int d^3 1\,\nabla_1^2 U(1)\nabla_1 V(1)$$
$$=-Ze\,[\nabla_1 V(1)]_{\mathbf{r}_1=\mathbf{R}(t_1)}\ , \tag{4}$$

since $\nabla_1^2 U(1)=-4\pi Ze\,\delta^{(3)}(\mathbf{r}_1-\mathbf{R}(t_1))$ for a moving particle of charge Ze. Considering a slab which confines Fermi-sea electrons with infinite-barrier bounding surfaces at $z=0$ and $z=L$ we denote vectors projected onto the x-y plane by subscripted parallel bars [e.g., $\mathbf{r}=(\mathbf{r}_\parallel,z)$], and introduce spatial Fourier transforms in the x-y plane of translational invariance. It is convenient at this point to also introduce an infinite three-dimensional (3D) Fourier transform of $U(2)$, despite spatial inhomogeneity in the z direction, with the result

$$\mathbf{f}=-(Ze)^2\left[\nabla_1\int_{-\infty}^{\infty}dz_2\int\frac{d\mathbf{q}_\parallel}{(2\pi)^2}e^{i\mathbf{q}_\parallel\cdot\mathbf{r}_1}\int_{-\infty}^{\infty}\frac{dq_z}{(2\pi)}e^{iq_z z_2}e^{-i(\mathbf{q}_\parallel\cdot\mathbf{R}_0+q_z z_0)}\right.$$
$$\left.\times e^{-i(\mathbf{q}_\parallel\cdot\mathbf{v}_\parallel+q_z v_z)t_1}\frac{K(z_1,z_2,\mathbf{q}_\parallel;\omega=\mathbf{q}_\parallel\cdot\mathbf{v}_\parallel+q_z v_z)}{\mathbf{q}_\parallel^2+q_z^2}\right]_{\mathbf{r}_1=\mathbf{v}t_1+\mathbf{R}_0}\ . \tag{5}$$

Breaking the frictional force $\mathbf{f}$ in Eq. (5) into components parallel and perpendicular to the surface of the slab, $\mathbf{f}=\mathbf{f}_\parallel+f_z\hat{\mathbf{k}}$, where $\hat{\mathbf{k}}$ is a unit vector perpendicular to the surface, we have

$$f_\parallel=-(Ze)^2\int_{-\infty}^{\infty}dz_2\int\frac{d\mathbf{q}_\parallel}{(2\pi)^2}iq_\parallel\int_{-\infty}^{\infty}\frac{dq_z}{(2\pi)}e^{iq_z z_2}e^{-iq_z z_0}e^{-iq_z v_z t_1}$$
$$\times\frac{K(z_1=v_z t_1+z_0,\,z_2;q_\parallel,\,\omega=\mathbf{q}_\parallel\cdot\mathbf{v}_\parallel+q_z v_z)}{q_\parallel^2+q_z^2} \tag{6}$$

and

$$f_z=-(Ze)^2\int_{-\infty}^{\infty}dz_2\int\frac{d\mathbf{q}_\parallel}{(2\pi)^2}\int_{-\infty}^{\infty}\frac{dq_z}{(2\pi)}\frac{e^{iq_z z_2}e^{-iq_z z_0}e^{-iq_z v_z t_1}}{q_\parallel^2+q_z^2}\left[\frac{\partial}{\partial z_1}K(z_1,z_2;q_\parallel,\,\omega=\mathbf{q}_\parallel\cdot\mathbf{v}_\parallel+q_z v_z)\right]_{z_1=v_z t_1+z_0}\ , \tag{7}$$

where $\mathbf{v}=\mathbf{v}_\parallel+v_z\hat{\mathbf{k}}$.

To carry out calculations for energy loss, we employ the inverse dielectric function for a finite slab of nonlocal dynamic solid-state plasma derived in a companion paper [Ref. 16(b)] in connection with a study of surface screening phenomena in a magnetic field. We shall draw upon the results of that analysis for various representations of $K(1,2)$ subject to the boundary condition of specular reflection of electrons at both slab faces, using those representations of

$K(1,2)$ which are convenient for our energy-loss calculations in a variety of conditions to be considered. One of the most useful forms of $K(1,2)$ is the *diagonal approximation* which neglects quantum interference effects associated with the vanishing of the wave functions and density at the infinite barrier boundaries,[17] while admitting to consideration bulk quantum effects arising in the temperature-dependent Lindhard dielectric function and its Landau quantized counterpart in high magnetic field. In this, only surface-induced spatially inhomogeneous modifications of the polarizability are ignored in the process of joining bulk dielectric response properties across the boundaries of adjoining media at the slab faces (including their complement of bulk quantum effects). For the *diagonal* approximation, we have for a slab with planar surfaces at $z=0$ and $z=L$,

$$
\begin{aligned}
K(z,z';q_{\parallel},\omega)=\theta(-z)\Bigg\{&\delta(z-z')-e^{q_{\parallel}z}\delta(z')+\frac{e^{q_{\parallel}z}}{2(1+\varepsilon_q)(1+\tilde{\varepsilon}_q)}[(2+\varepsilon_q+\tilde{\varepsilon}_q)\delta(z')+(\varepsilon_q-\tilde{\varepsilon}_q)\delta(L-z')]\\
&+\theta(z')\theta(L-z')e^{q_{\parallel}z}\left[\frac{\tilde{\varepsilon}_q}{1+\tilde{\varepsilon}_q}\frac{2}{L}\sum_{q_z(\text{even})}\frac{\eta_q\cos(q_zz')}{\varepsilon_L(\mathbf{q},\omega)}+\frac{\varepsilon_q}{1+\varepsilon_q}\frac{2}{L}\sum_{q_z(\text{odd})}\frac{\cos(q_zz')}{\varepsilon_L(\mathbf{q},\omega)}\right]\Bigg\}\\
+\theta(z)\theta(L-z)\Bigg\{&-[\delta(L-z')-\delta(z')]\frac{\varepsilon_q}{1+\varepsilon_q}\frac{2q_{\parallel}}{L}\sum_{q_z(\text{odd})}\frac{\cos(q_zz)}{|\mathbf{q}|^2\varepsilon_L(\mathbf{q},\omega)}\\
&+[\delta(L-z')+\delta(z')]\frac{\tilde{\varepsilon}_q}{1+\tilde{\varepsilon}_q}\frac{2q_{\parallel}}{L}\sum_{q_z(\text{even})}\frac{\eta_q\cos(q_zz)}{|\mathbf{q}|^2\varepsilon_L(\mathbf{q},\omega)}\\
&+\theta(z')\theta(L-z')\Bigg[\frac{2}{L}\sum_{q_z(\text{odd})}\frac{\cos(q_zz)\cos(q_zz')}{\varepsilon_L(\mathbf{q},\omega)}+\frac{2}{L}\sum_{q_z(\text{even})}\frac{\eta_q\cos(q_zz)\cos(q_zz')}{\varepsilon_L(\mathbf{q},\omega)}\\
&-\frac{\varepsilon_q}{1+\varepsilon_q}\frac{8q_{\parallel}}{L^2}\sum_{q_z(\text{odd})}\frac{\cos(q_zz)}{|\mathbf{q}|^2\varepsilon_L(\mathbf{q},\omega)}\sum_{k_z(\text{odd})}\frac{\cos(k_zz')}{\varepsilon_L(\mathbf{k},\omega)}\\
&-\frac{\tilde{\varepsilon}_q}{1+\tilde{\varepsilon}_q}\frac{8q_{\parallel}}{L^2}\sum_{q_z(\text{even})}\eta_q\frac{\cos(q_zz)}{|\mathbf{q}|^2\varepsilon_L(\mathbf{q},\omega)}\sum_{k_z(\text{even})}\eta_k\frac{\cos(k_zz')}{\varepsilon_L(\mathbf{k},\omega)}\Bigg]\Bigg\}\\
+\theta(z-L)\Bigg\{&\delta(z-z')-e^{-q_{\parallel}(z-L)}\delta(L-z')+\frac{e^{-q_{\parallel}(z-L)}}{2(1+\varepsilon_q)(1+\tilde{\varepsilon}_q)}[(2+\varepsilon_q+\tilde{\varepsilon}_q)\delta(L-z')+(\varepsilon_q-\tilde{\varepsilon}_q)\delta(z')]\\
&+\theta(z')\theta(L-z')e^{q_{\parallel}(L-z)}\left[\frac{\tilde{\varepsilon}_q}{1+\tilde{\varepsilon}_q}\frac{2}{L}\sum_{q_z(\text{even})}\frac{\eta_q\cos(q_zz')}{\varepsilon_L(\mathbf{q},\omega)}-\frac{\varepsilon_q}{1+\varepsilon_q}\frac{2}{L}\sum_{q_z(\text{odd})}\frac{\cos(q_zz')}{\varepsilon_L(\mathbf{q},\omega)}\right]\Bigg\}.
\end{aligned}
\tag{8}
$$

In this notation, $q_z=n\pi/L$ where $n=0,1,2,\ldots,\infty$ and $\eta_{q_z}=\frac{1}{2}$ for $q_z=0$ and 1 for $q_z>0$, and the vector $\mathbf{k}$ has components k_z and $\mathbf{q}_{\parallel}$. $\theta(x)$ is the Heaviside step function. Also,

$$
\varepsilon_q^{-1}(\omega)\equiv\frac{4q_{\parallel}}{L}\sum_{q_z(\text{odd})}\frac{1}{|\mathbf{q}|^2\varepsilon_L(\mathbf{q},\omega)}\ , \tag{9a}
$$

and

$$
\tilde{\varepsilon}_q^{-1}(\omega)\equiv\frac{4q_{\parallel}}{L}\sum_{q_z(\text{even})}\frac{\eta_{q_z}}{|\mathbf{q}|^2\varepsilon_L(\mathbf{q},\omega)}\ , \tag{9b}
$$

where $\varepsilon_L(\mathbf{q},\omega)$ is the wave-number- and frequency-dependent dielectric function for an infinite solid. It will generally be approximated in the random-phase approximation in this work. The diagonal approximation may be expected to be useful for samples which are large in comparison with the characteristic distance over which surface-induced spatial inhomogeneities penetrate the polarization properties, $L\gg 1/2k_F$. Moreover, the diagonal approximation is also valid in any classical or semiclassical description of nonlocal response.

III. PARTICLE MOTION PARALLEL TO THE SLAB SURFACES: HIGH-VELOCITY LIMIT

Considering parallel motion of a charged particle at a distance z_0 from the surface, with velocity $v_\parallel$ ($v_z=0$), the *stopping power* (energy loss per unit path length) is given by $S\equiv v^{-1}dW/dt$, where the rate at which the charged particle loses energy is

$$\frac{dW}{dt}=\mathbf{f}\cdot\mathbf{v}\ . \tag{10}$$

Using Eq. (6) with $\tilde{z}_2=z_2-z_0$, we find

$$S=-i\frac{Ze^2}{v}\int d\tilde{z}_2\int\frac{d\bar{q}_\parallel}{2\pi}\frac{\bar{v}\cdot\bar{q}_\parallel}{q_\parallel}e^{-q_\parallel\tilde{z}_2}K(z_1=z_0,\,z_2=\tilde{z}_2+z_0;q_\parallel,\,\omega=q_\parallel\cdot\mathbf{v}) \tag{11a}$$

or, alternatively,

$$S=\frac{-i(Ze)^2}{(2\pi)^2 v}\int_{-\infty}^{\infty}dq_x\int_{-\infty}^{\infty}dq_y\,\mathbf{v}\cdot\mathbf{q}_\parallel V(z_0,z_0;q_\parallel,\,\omega=q_\parallel\cdot\mathbf{v})\ . \tag{11b}$$

Here, $V(z,z',q_\parallel;\omega)$ is the electrostatic potential at z due to a Coulomb charge of unit strength at z', taking full account of the dynamic nonlocal polarization of the dielectric slab. After a lengthy but straightforward calculation, making use of the diagonal approximation of Eq. (8), we have obtained the value of $V(z,z';q_\parallel,\omega)$ for (a) the cross-boundary situation, i.e., when z and z' are on opposite sides of a surface of the slab, with one of the test charges inside the slab, (b) when z and z' are both in the vacuum region, and (c) when z and z' are both inside the slab. Substituting these results into Eq. (11), we obtain the energy loss per unit path length for a particle *outside* the slab at a distance z_0 from the surface as

$$\begin{aligned}S=\frac{i(Ze)^2}{2\pi v}\int_{-\infty}^{\infty}dq_x\int_{-\infty}^{\infty}dq_y\frac{\mathbf{v}\cdot\mathbf{q}_\parallel}{q_\parallel}e^{-2q_\parallel z_0}\Bigg\{&1-\frac{2+\varepsilon_q+\tilde{\varepsilon}_q}{(1+\varepsilon_q)(1+\tilde{\varepsilon}_q)}-\frac{\varepsilon_q-\tilde{\varepsilon}_q}{2(1+\varepsilon_q)(1+\tilde{\varepsilon}_q)}e^{-q_\parallel L}\\&+\frac{e^{-q_\parallel L}}{1+\tilde{\varepsilon}_q^{-1}}\frac{2}{L}\sum_{q_z(\text{even})}\frac{\eta_{q_z}}{|\mathbf{q}|^2\varepsilon_L(\mathbf{q},\,\mathbf{q}_\parallel\cdot\mathbf{v})}[q_\parallel\cos(q_zL)-q_z\sin(q_zL)]\\&+\frac{e^{-q_\parallel L}}{1+\varepsilon_q^{-1}}\frac{2}{L}\sum_{q_z(\text{odd})}\frac{1}{|\mathbf{q}|^2\varepsilon_L(\mathbf{q},\,\mathbf{q}_\parallel\cdot\mathbf{v})}[q_\parallel\cos(q_zL)-q_z\sin(q_zL)]\Bigg\}\ .\end{aligned} \tag{12}$$

For a particle traveling *inside* the slab at a distance z_0 from the surface, our calculations show that the energy loss per unit path length is obtained by substituting the following result for the electrostatic potential for $0<z,z'<L$ into Eq. (11):

$$\begin{aligned}V(z,z';q_\parallel,\omega)\Big/\left[\frac{2\pi e^2}{q_\parallel}\right]&=e^{-q_\parallel(L-z')}\left[\frac{1}{1+\tilde{\varepsilon}_q^{-1}}\frac{2q_\parallel}{L}\sum_{q_z(\text{even})}\eta_{q_z}\frac{\cos(q_zz)}{|\mathbf{q}|^2\varepsilon_L(\mathbf{q},\omega)}-\frac{1}{1+\varepsilon_q^{-1}}\frac{2q_\parallel}{L}\sum_{q_z(\text{odd})}\frac{\cos(q_zz)}{|\mathbf{q}|^2\varepsilon_L(\mathbf{q},\omega)}\right]\\&+\frac{2}{L}\sum_{q_z(\text{odd})}\frac{\cos(q_zz)}{|\mathbf{q}|^2\varepsilon_L(\mathbf{q},\omega)}\{2q_\parallel\cos(q_zz')-e^{-q_\parallel(L-z')}[q_\parallel\cos(q_zL)-q_z\sin(q_zL)]\}\\&+\frac{2}{L}\sum_{q_z(\text{even})}\eta_{q_z}\frac{\cos(q_zz)}{|\mathbf{q}|^2\varepsilon_L(\mathbf{q},\omega)}\{2q_\parallel\cos(q_zz')-e^{-q_\parallel(L-z')}[q_\parallel\cos(q_zL)-q_z\sin(q_zL)]\}\\&-\frac{1}{1+\varepsilon_q^{-1}}\frac{8q_\parallel}{L^2}\sum_{q_z(\text{odd})}\frac{\cos(q_zz)}{|\mathbf{q}|^2\varepsilon_L(\mathbf{q},\omega)}\sum_{k_z(\text{odd})}\frac{1}{|\mathbf{k}|^2\varepsilon_L(\mathbf{k},\omega)}\{2q_\parallel\cos(k_zz')-q_\parallel e^{-q_\parallel z'}\\&-e^{-q_\parallel(L-z')}[q_\parallel\cos(k_zL)-k_z\sin(k_zL)]\}\\&-\frac{1}{1+\tilde{\varepsilon}_q^{-1}}\frac{8q_\parallel}{L^2}\sum_{q_z(\text{even})}\frac{\eta_{q_z}\cos(q_zz)}{|\mathbf{q}|^2\varepsilon_L(\mathbf{q},\omega)}\sum_{k_z(\text{even})}\frac{\eta_{k_z}}{|\mathbf{k}|^2\varepsilon_L(\mathbf{k},\omega)}\{2q_\parallel\cos(k_zz')-q_\parallel e^{-q_\parallel z'}\\&-e^{-q_\parallel(L-z')}[q_\parallel\cos(k_zL)-k_z\sin(k_zL)]\}\ ,\end{aligned} \tag{13}$$

where the wave vector $\mathbf{k}$ has components k_z and $\mathbf{q}_\parallel$. In the limit of high velocity, when the dielectric function $\varepsilon(\mathbf{q},\omega)$ is

taken to be independent of wave number and equal to the local limit $\varepsilon(\omega)$, we have $\varepsilon_q=\varepsilon(\omega)\coth(q_\parallel L/2)$ and $\tilde{\varepsilon}_q=\varepsilon(\omega)\tanh(q_\parallel L/2)$ (null magnetic field). Substituting these results into Eqs. (13) and (11), and taking the *thick* film limit $L\to\infty$, we find that the stopping power for an electron traveling *inside* the slab at a distance z_0 from the surface is given by

$$S\approx\frac{(Ze)^2\omega_p^2}{v^2}\ln\left\{\frac{k_c v}{\omega_p}+\left[1+\left[\frac{k_c v}{\omega_p}\right]^2\right]^{1/2}\right\}+\frac{(Ze)^2\omega_s^2}{v^2}K_0\left[\frac{2\omega_s z_0}{v}\right]-\frac{(Ze)^2\omega_p^2}{v^2}K_0\left[\frac{2\omega_p z_0}{v}\right]$$
$$+2\frac{(Ze)^2\omega_p^2}{v^2}K_0\left[\frac{\omega_p L}{v}\right]-\frac{(Ze)^2\omega_s^2}{v^2}K_0\left[\frac{\omega_s L}{v}\right], \tag{14}$$

where ω_p is the bulk plasma frequency and $\omega_s\equiv\omega_p/\sqrt{2}$ is the frequency of the surface plasmon in the long-wavelength limit. $K_0(x)$ is a Bessel function of imaginary argument, k_c is a cutoff wave number associated with the onset of natural damping which has been introduced into the bulk contribution to the stopping power, which ensures that the result is finite. The first three terms have been calculated by Núñez, Echenique, and Ritchie[12] for the half-space geometry. The last two terms in Eq. (14) are due to the finite slab thickness.

IV. PARTICLE MOTION PENETRATING ACROSS A PLASMA SLAB: HIGH-VELOCITY LIMIT

We consider a charged particle penetrating across a slab, normal to its bounding surfaces at a constant velocity throughout, neglecting the change of speed upon entering and leaving the binding potential of the quantum well. In this approximation, the force on the charged particle is, from Eq. (7) ($v_\parallel=0$),

$$f_z=-(Ze)^2\int_{-\infty}^{\infty}dz_2\int\frac{d^2\mathbf{q}_\parallel}{(2\pi)^2}\int_{-\infty}^{\infty}\frac{dq_z}{2\pi}\frac{e^{iq_z(z_2-z_0-v_z t_1)}}{q_\parallel^2+q_z^2}\frac{\partial}{\partial z_0}K(z_0+v_z t_1,\,z_2;q_\parallel,\,\omega=q_z v_z)\,. \tag{15}$$

Forming the total work integral

$$W=\int_{-\infty}^{\infty}dz_0\,f_z \tag{16}$$

and integrating by parts with respect to z_0, we obtain (set $\tilde{z}_0=z_0+v_z t_1$)

$$W=-(Ze)^2\int_{-\infty}^{\infty}dz_2\int_{-\infty}^{\infty}d\tilde{z}_0\int\frac{d^2q_\parallel}{(2\pi)^2}\int_{-\infty}^{\infty}\frac{dq_z}{2\pi}q_z\frac{e^{iq_z z_2}e^{-iq_z\tilde{z}_0}}{q_\parallel^2+q_z^2}\mathrm{Im}K(\tilde{z}_0,z_2;q_\parallel,\,\omega=q_z v_z)\,, \tag{17}$$

where Im stands for the imaginary part. Alternatively, putting $\omega=q_z v_z$, we obtain

$$W=\int d^2\mathbf{q}_\parallel\int_{-\infty}^{\infty}d\omega\,\hbar\omega P(q_\parallel,\omega)\,, \tag{18}$$

where the probability function is defined by[1]

$$P(q_\parallel,\omega)=\frac{1}{\hbar}\frac{(Ze)^2}{2\pi^2}\frac{1}{q_\parallel^2v^2+\omega^2}\int_{-\infty}^{\infty}d\tilde{z}_0\int_{-\infty}^{\infty}dz_2\,e^{-i\tilde{z}_0\omega/v}\mathrm{Im}K(\tilde{z}_0,z_2;q_\parallel,\omega)e^{iz_2\omega/v}\,. \tag{19}$$

In this, we have used the fact that the imaginary part of the inverse dielectric function is an odd function of ω and the real part is an even function of ω. The representation for energy loss in Eq. (17) is useful for carrying out calculations in the low-velocity limit.

For a particle crossing a 2D inversion layer sheet at the $z=0$ plane, we have[18]

$$\mathrm{Im}K(\tilde{z}_0,z_2;q_\parallel,\omega)=\delta(z_2)e^{-|\mathbf{q}_\parallel||\tilde{z}_0|}\mathrm{Im}K^{2D}(q_\parallel,\omega)\,, \tag{20}$$

where $K^{2D}(q_\parallel,\omega)$ is the reciprocal of the dielectric function of a two-dimensional electron gas. Substituting Eq. (20) into Eq. (17) yields

$$W_{2D}=(Ze)^2\int\frac{d^2q_\parallel}{(2\pi)^2}\int_{-\infty}^{\infty}\frac{dq_z}{2\pi}\frac{2q_z|\mathbf{q}_\parallel|}{(|\mathbf{q}_\parallel|^2+q_z^2)^2}\mathrm{Im}K^{2D}(q_\parallel,\,\omega=q_z v_z)\,. \tag{21}$$

In this very-thin-film limit, when only the lowest subband is taken into account for the heterostructure, the formal result for energy loss is relatively simple.

To proceed further with the determination of energy loss to a slab of finite thickness, we employ the inverse dielectric function $K(z,z';q_\parallel,\omega)$ given in Eq. (8). Our calculation based upon the diagonal approximation of Eq. (8) yields

$$P(q_\parallel,\omega)\equiv\frac{(Ze)^2}{2\pi^2\hbar v^2}\frac{1}{q_\parallel^2+\omega^2/v^2}\mathrm{Im}(U)\,, \tag{22}$$

where U is given by

$$U \equiv \frac{1}{q_\parallel^2+\omega^2/v^2}\left\{\frac{q_\parallel\{\varepsilon_q[\cos(\omega L/v)-1]-\tilde{\varepsilon}_q[\cos(\omega L/v)+1]-2\varepsilon_q\tilde{\varepsilon}_q\}}{(1+\varepsilon_q)(1+\tilde{\varepsilon}_q)}\right.$$
$$+\frac{\tilde{\varepsilon}_q}{1+\tilde{\varepsilon}_q}\frac{8q_\parallel\omega}{vL}\sin\left[\frac{\omega L}{v}\right]\sum_{q_z(\text{even})}\frac{\eta_{q_z}}{\varepsilon_L(\mathbf{q},\omega)}\frac{1}{(\omega/v)^2-q_z^2}$$
$$-\frac{\varepsilon_q}{1+\varepsilon_q}\frac{8q_\parallel\omega}{vL}\sin\left[\frac{\omega L}{v}\right]\sum_{q_z(\text{odd})}\frac{1}{\varepsilon_L(\mathbf{q},\omega)}\frac{1}{(\omega/v)^2-q_z^2}$$
$$+\frac{4}{L}\left[\frac{\omega}{v}\right]^2\left[\cos\left[\frac{\omega L}{v}\right]-1\right]\sum_{q_z(\text{even})}\frac{\eta_{q_z}}{\varepsilon_L(\mathbf{q},\omega)}\frac{1}{(\omega/v)^2-q_z^2}$$
$$\left.-\frac{4}{L}\left[\frac{\omega}{v}\right]^2\left[\cos\left[\frac{\omega L}{v}\right]+1\right]\sum_{q_z(\text{odd})}\frac{1}{\varepsilon_L(\mathbf{q},\omega)}\frac{1}{(\omega/v)^2-q_z^2}\right\}$$
$$+\frac{4}{L}\left[\frac{\omega}{v}\right]^2\left[1+\cos\left[\frac{\omega L}{v}\right]\right]\sum_{q_z(\text{odd})}\frac{1}{\varepsilon_L(\mathbf{q},\omega)[(\omega/v)^2-q_z^2]^2}$$
$$+\frac{4}{L}\left[\frac{\omega}{v}\right]^2\left[1-\cos\left[\frac{\omega L}{v}\right]\right]\sum_{q_z(\text{even})}\eta_{q_z}\frac{1}{\varepsilon_L(\mathbf{q},\omega)[(\omega/v)^2-q_z^2]^2}$$
$$-\left[\frac{4\omega}{Lv}\right]^2 q_\parallel\frac{1}{q_\parallel^2+\omega^2/v^2}\left[\frac{\varepsilon_q}{1+\varepsilon_q}[1+\cos(\omega L/v)]\left[\sum_{q_z(\text{odd})}\frac{1}{\varepsilon_L(\mathbf{q},\omega)}\frac{1}{(\omega/v)^2-q_z^2}\right]^2\right.$$
$$\left.+\frac{\tilde{\varepsilon}_q}{1+\tilde{\varepsilon}_q}[1-\cos(\omega L/v)]\left[\sum_{q_z(\text{even})}\eta_{q_z}\frac{1}{\varepsilon_L(\mathbf{q},\omega)}\frac{1}{(\omega/v)^2-q_z^2}\right]^2\right]. \tag{23}$$

These results provide a complete description of the energy loss of a charged particle passing through a slab of dielectric material where *both* the wave-number and frequency dependencies of the dielectric response function are taken into account, within the framework of the diagonal approximation assuming classical specular scattering at the surfaces. It is straightforward to show that in the high-velocity limit $q\to 0$ we obtain the well-known result of Ritchie.[1] Taking $\varepsilon_L(\mathbf{q},\omega)$ to be the local dielectric function $\varepsilon(\omega)\equiv\varepsilon$ and using the relations

$$\sum_{q_z(\text{odd})}\frac{1}{\alpha-q_z^2}=-\frac{L}{4\alpha^{1/2}}\tan\left[\frac{L}{2}\alpha^{1/2}\right], \tag{24a}$$

$$\sum_{q_z(\text{even})}\frac{\eta_{q_z}}{\alpha-q_z^2}=\frac{L}{4\alpha^{1/2}}\cot\left[\frac{L}{2}\alpha^{1/2}\right]. \tag{24b}$$

Taken jointly with $\varepsilon_q=\varepsilon\coth(q_\parallel L/2)$ and $\tilde{\varepsilon}_q=\varepsilon\tanh(q_\parallel L/2)$ these results yield the probability function in the local limit of dielectric response as (no magnetic field and no phonons)

$$P(q_\parallel,\omega)=\frac{(Ze)^2}{2\pi^2\hbar v^2}\left[\text{Im}\left[\frac{1}{\varepsilon}\right]\frac{L}{q_\parallel^2+\omega^2/v^2}\right.$$
$$\left.+\frac{2q_\parallel}{(q_\parallel^2+\omega^2/v^2)^2}\text{Im}\left[\frac{1-\varepsilon}{\varepsilon}\frac{2(\varepsilon-1)\cos(\omega L/v)+(\varepsilon-1)^2e^{q_\parallel L}+(1-\varepsilon^2)e^{q_\parallel L}}{(\varepsilon-1)^2e^{-q_\parallel L}-(\varepsilon+1)^2e^{-q_\parallel L}}\right]\right] \tag{25}$$

(which is appropriate in the high-velocity limit since $\omega=q_z v_z$).

In the *thick*-slab limit, i.e., $q_\parallel L \gg 1$, Eq. (25) becomes[1]

$$P(q_\parallel,\omega)\approx LP'_\infty(q_\parallel,\omega)+P_b(q_\parallel,\omega)\ , \tag{26a}$$

where

$$P'_\infty(q_\parallel,\omega)\equiv\frac{(Ze)^2}{\pi^2\hbar v^2}\frac{1}{q_\parallel^2+\omega^2/v^2}\mathrm{Im}\left[\frac{1}{\varepsilon}\right]\ , \tag{26b}$$

$$P_b(q_\parallel,\omega)\equiv\frac{2(Ze)^2 q_\parallel}{\pi^2\hbar v^2}\frac{1}{(q_\parallel^2+\omega^2/v^2)^2}\mathrm{Im}\left[\frac{(1-\varepsilon)^2}{\varepsilon(1+\varepsilon)}\right]\ . \tag{26c}$$

Specifically, with $\varepsilon(\omega)=\varepsilon=1-\omega_p^2/(\omega^2-i0^+)$ we obtain

$$P_b(q_\parallel,\omega)=\frac{2(Ze)^2 q_\parallel}{\pi\hbar v^2}\frac{\pi\omega_p^2/\omega}{(q_\parallel^2+\omega^2/v^2)^2}\times\left[\delta\left[\frac{\omega^2-\omega_s^2}{\omega}\right]-\delta\left[\frac{\omega^2-\omega_p^2}{\omega}\right]\right] \tag{27a}$$

and

$$P'_\infty(q_\parallel,\omega)\equiv\frac{(Ze)^2}{\pi\hbar v^2}\frac{\omega_p^2}{q_\parallel^2+\omega^2/v^2}\delta(\omega^2-\omega_p^2)\ . \tag{27b}$$

Integrating this in accordance with Eq. (18) to obtain the total work done, $W\equiv W_{\mathrm{bulk}}+W_{\mathrm{surf}}$, where the bulk and surface terms are, respectively,

$$W_{\mathrm{bulk}}=\frac{L(Ze)^2\omega_p^2}{v^2}\ln\left[1+\left[\frac{\kappa v}{\omega_p}\right]^2\right] \tag{28a}$$

$$W_{\mathrm{surf}}=\frac{\pi(Ze)^2\omega_s}{v}\left[1-\frac{1}{\sqrt{2}}\right]\ . \tag{28b}$$

Taking the cutoff wave number $\kappa=\omega_p/v$, we obtain $W_{\mathrm{bulk}}/W_{\mathrm{surf}}=1.065t$, where $t\equiv\omega_p L/v$. In the experiments carried out in Refs. 9 and 10, we have $L=650$ Å, $v=10^8$ cm sec^{-1} and $\omega_p=2.13\times10^{14}$ sec^{-1} so that $W_{\mathrm{bulk}}/W_{\mathrm{surf}}\approx14.8$, and the surface terms may be neglected in analyzing the data.

V. LOW-VELOCITY LIMIT FOR PARTICLE CROSSING PLASMA SLAB

The low-velocity limit for energy loss is amenable to analysis. For charged particles moving perpendicular to the surfaces of the slab, we may obtain the low-velocity limit of W by expanding the inverse dielectric function K in Eq. (17) to linear order in $\omega=q_z v_z$, while holding the nonlocal dispersive structure of K intact. This yields

$$W=v_z(Ze)^2\int_{-\infty}^{\infty}dz_2\int_{-\infty}^{\infty}d\bar{z}_0\int\frac{d^2q_\parallel}{(2\pi)^2}\int_{-\infty}^{\infty}\frac{dq_z}{2\pi}q_z^2\frac{e^{iq_z z_2}e^{-iq_z\bar{z}_0}}{q_\parallel^2+q_z^2}\left[\mathrm{Im}\frac{\partial}{\partial\omega}K(\bar{z}_0,z_2;q_\parallel,\omega\right]_{\omega=0}\ , \tag{29}$$

and carrying out the q_z integral explicitly in Eq. (29), we have

$$W=-\frac{v_z}{2}(Ze)^2\int_{-\infty}^{\infty}dz_2\int_{-\infty}^{\infty}d\bar{z}_0\int\frac{d^2q_\parallel}{(2\pi)^2}|\mathbf{q}_\parallel|^2 e^{-|\mathbf{q}_\parallel||z_2-\bar{z}_0|}\left[\mathrm{Im}\frac{\partial}{\partial\omega}K(\bar{z}_0,z_0;q_\parallel,\omega)\right]_{\omega=0}\ . \tag{30}$$

Considering the situation when screening effects are weak (low phonon density), the RPA integral equation

$$K(1,2)=\delta^4(1-2)+\int d^4 3\int d^4 4\, v(1-3)R(3,4)K(4,2) \tag{31}$$

reduces to the ordinary Hartree-Fock approximation

$$K_{\mathrm{HF}}(1,2)=\delta^4(1-2)+\int d^4 3\, v(1-3)R(3,2)\ , \tag{32}$$

where $R(1,2)$ is the density perturbation response function

$$R(1,2)\equiv\frac{\delta\rho(1)}{\delta V(2)}=-i\bar{G}_1(1,2)\bar{G}_1(2,1^+)\ . \tag{33}$$

[$\bar{G}_1(1,2)$ is the one-electron thermodynamic Green's function and $R(1,2)$ is the ring-diagram contribution of density-density response; $v(1-2)$ is the Coulomb potential.] For a single quantum well with transverse subband wave functions $u_\alpha(z)$, we have quite generally

$$R(z_1,z_2;q_\parallel,\omega)=\sum_\alpha u_\alpha(z_1)u_\alpha^*(z_2)u_\beta(z_2)\times u_\beta^*(z_1)R^{\mathrm{2D}}_{\alpha\beta}(q_\parallel,\omega)\ , \tag{34}$$

where

$$R^{\mathrm{2D}}_{\alpha\beta}(q,\omega)=2\int\frac{dk}{2\pi}\frac{f(\varepsilon_k+E_\alpha)-f(\varepsilon_{k-q}+E_\beta)}{\hbar\omega+\varepsilon_k+E_\alpha-\varepsilon_{k-q}-E_\beta+i0^+}\ . \tag{35}$$

In this, $f(\varepsilon)$ is the Fermi-Dirac distribution function and ε_k+E_α is the electron energy in the αth subband, where $\varepsilon_k=\hbar^2k^2/2m^*$ with m^* equal to the electron effective mass. Employing the unscreened approximation of Eq. (32) for K in Eq. (30), and carrying out the $\bar{z}_0$ integral, we obtain W as

$$W=-\frac{v_z(Ze)^2}{2}\sum_\alpha\int_0^\infty dq_\parallel\,|q_\parallel|\left[\mathrm{Im}\frac{\partial}{\partial\omega}R^{\mathrm{2D}}_{\alpha\alpha}(q_\parallel,\omega)\right]_{\omega=0}\times\left[1-|q_\parallel|\frac{\partial}{\partial|q_\parallel|}\right]F_\alpha(q_\parallel)\ , \tag{36}$$

where we have used the following approximation for a quantum well:

$$\int_{-\infty}^{\infty} dz_2 \int_{-\infty}^{\infty} dz_3\, u_\alpha^*(z_2) u_\beta(z_2) e^{-|q_\parallel||z_2-z_3|} u_\beta^*(z_3) u_\alpha(z_3) \approx \delta_{\alpha\beta} \int_{-\infty}^{\infty} dz_2 \int_{-\infty}^{\infty} dz_3\, |u_\alpha(z_2)|^2 e^{-|q_\parallel||z_2-z_3|} |u_\alpha(z_3)|^2 \equiv \delta_{\alpha\beta} F_\alpha(q_\parallel) \,. \quad (37)$$

It is readily recognized that $R_{\alpha\alpha}^{2D}(q_\parallel,\omega)$ is the two-dimensional density perturbation response function with chemical potential measured relative to the subband energy E_α. $R_{\alpha\alpha}^{2D}(q_\parallel,\omega)$ is well known both in the presence and absence of a magnetic field,[19] and it is straightforward to obtain W by numerical integration of Eq. (36) for any regime of temperature, with slight modification of the formula to accommodate a magnetic field having a discrete 2D energy spectrum in place of $\varepsilon \to n\hbar\omega_c$. The special case of a field-free nondegenerate 2D quantum plasma in highly tractable with

$$\mathrm{Im} R_{\alpha\alpha}^{2D}(q_\parallel,\omega) = \frac{\rho^{2D}}{8\pi} \left[\frac{8\pi\beta m^*}{q_\parallel^2} \right]^{1/2} \exp\left[\frac{-\beta q_\parallel^2}{8m^*} \right] \times \sinh(\beta\omega) \exp\left[\frac{-\beta m^* \omega^2}{4q_\parallel^2} \right] , \quad (38)$$

and correspondingly

$$\left[\mathrm{Im} \frac{\partial}{\partial\omega} R_{\alpha\alpha}^{2D}(q_\parallel,\omega) \right]_{\omega=0} = \frac{\beta\rho^{2D}}{8\pi} \left[\frac{8\pi\beta m^*}{q_\parallel^2} \right]^{1/2} \exp\left[\frac{-\beta q_\parallel^2}{8m^*} \right] , \quad (39)$$

where $\beta = 1/k_B T$ and the nondegenerate areal density for the 2D electron gas is $\rho^{2D} = 4m^* e^{\beta\zeta_\alpha}/\beta$. ($\zeta_\alpha$ is the chemical potential relative to the subband energy E_α.)

VI. MAGNETOPLASMON-PHONON EFFECTS ON ENERGY LOSS AT HIGH VELOCITY

In addition to accommodating nonlocal dispersive effects, our formulation can easily incorporate the role of dynamic phonon polarization and magnetic field effects in the plasma (magnetopolariton) energy loss of a charged particle to a finite slab of dielectric material. In particular, we treat the energy loss in the high-velocity limit, again employing the *diagonal approximation* of the inverse dielectric function $K(1,2)$. The Landau quantized Lindhard dielectric function for the bulk system in the long-wavelength limit is given by the following classical result which incorporates the dynamic phonon polarization:[20]

$$\varepsilon_L(\mathbf{q},\omega) = \varepsilon_\infty \left[1 + \frac{\Omega^2}{\omega_{TO}^2 - \omega^2} \right] \times \left[1 - \frac{q_z^2}{q^2\omega^2} [\Omega_p(\omega)]^2 - \frac{q_\parallel^2}{q^2} \frac{[\Omega_p(\omega)]^2}{\omega^2 - \omega_c^2} \right] , \quad (40)$$

where it is understood that ω^2 has a small negative imaginary part, i.e., $\omega^2 \to \omega^2 - i0^+$, ε_∞ is the high-frequency dielectric constant, ω_c is the cyclotron frequency, $\Omega^2 \equiv \omega_{LO}^2 - \omega_{TO}^2$, with ω_{TO} and ω_{LO} as the transverse optical and longitudinal optical phonon frequencies, respectively, and

$$[\Omega_p(\omega)]^2 = \frac{\omega_p^2}{\varepsilon_\infty \left[1 + \frac{\Omega^2}{\omega_{TO}^2 - \omega^2} \right]} \,. \quad (41)$$

Here $\omega_p^2 \equiv 4\pi e^2 \rho / m^*$ is the square of the bulk plasma frequency, ρ is the electron bulk density, and m^* is the electron effective mass. Substituting Eq. (40) into Eqs. (9) and carrying out the sums with the use of Eqs. (24), we obtain the results

$$\sum_{q_z(\mathrm{odd})} \frac{1}{|\mathbf{q}|^2 \varepsilon_L(\mathbf{q},\omega)} = \frac{L/4q_\parallel}{\varepsilon_\infty \left[1 + \frac{\Omega^2}{\omega_{TO}^2 - \omega^2} \right]} \left[1 - \frac{[\Omega_p(\omega)]^2}{\omega^2} \right]^{-1/2} \left[1 - \frac{[\Omega_p(\omega)]^2}{\omega^2 - \omega_c^2} \right]^{-1/2} \times \tanh\left[\frac{q_\parallel L}{2} \left[\frac{1 - [\Omega_p(\omega)]^2/(\omega^2 - \omega_c^2)}{1 - [\Omega_p(\omega)]^2/\omega^2} \right]^{1/2} \right] , \quad (42)$$

$$\sum_{q_z(\mathrm{even})} \frac{\eta_{q_z}}{|\mathbf{q}|^2 \varepsilon_L(\mathbf{q},\omega)} = \frac{L/4q_\parallel}{\varepsilon_\infty \left[1 + \frac{\Omega^2}{\omega_{TO}^2 - \omega^2} \right]} \left[1 - \frac{[\Omega_p(\omega)]^2}{\omega^2} \right]^{-1/2} \left[1 - \frac{[\Omega_p(\omega)]^2}{\omega^2 - \omega_c^2} \right]^{-1/2} \times \coth\left[\frac{q_\parallel L}{2} \left[\frac{1 - [\Omega_p(\omega)]^2/(\omega^2 - \omega_c^2)}{1 - [\Omega_p(\omega)]^2/\omega^2} \right]^{1/2} \right] , \quad (43)$$

$$\sum_{q_z(\text{odd})} \frac{1}{\varepsilon_L(\mathbf{q},\omega)} \frac{1}{(\omega/v)^2-q_z^2} = \tilde{C}(\omega) \left[\frac{L}{4\Gamma} \tanh\left[\frac{\Gamma L}{2}\right] \left[\frac{\Gamma^2-q_\parallel^2}{\Gamma^2+(\omega/v)^2}\right] + \frac{L}{4\omega/v} \left[\frac{q_\parallel^2+(\omega/v)^2}{\Gamma^2+(\omega/v)^2}\right] \tan\left[\frac{\omega L}{2v}\right] \right], \tag{44}$$

$$\sum_{q_z(\text{even})} \frac{\eta_{q_z}}{\varepsilon_L(\mathbf{q},\omega)} \frac{1}{(\omega/v)^2-q_z^2} = \tilde{C}(\omega) \left[\frac{L}{4\Gamma} \coth\left[\frac{\Gamma L}{2}\right] \left[\frac{\Gamma^2-q_\parallel^2}{\Gamma^2+(\omega/v)^2}\right] - \frac{L}{4\omega/v} \left[\frac{q_\parallel^2+(\omega/v)^2}{\Gamma^2+(\omega/v)^2}\right] \cot\left[\frac{\omega L}{2v}\right] \right], \tag{45}$$

where

$$\tilde{C}(\omega) \equiv \frac{1}{\varepsilon_\infty \left[1+\frac{\Omega^2}{\omega_{\text{TO}}^2-\omega^2}\right]} \frac{1}{\left[\frac{[\Omega_p(\omega)]^2}{\omega^2}-1\right]} = -\frac{1}{\varepsilon_\infty - \frac{\omega_p^2}{\omega^2} + \frac{\Omega^2}{\omega_{\text{TO}}^2-\omega^2}} \tag{46}$$

and

$$\Gamma(\omega,q_\parallel;\omega_c) \equiv q_\parallel \left[\frac{1-\frac{[\Omega_p(\omega)]^2}{\omega^2-\omega_c^2}}{1-\frac{[\Omega_p(\omega)]^2}{\omega^2}} \right]^{1/2} . \tag{47}$$

Clearly $\Gamma = q_\parallel$ for $\omega_c = 0$ (i.e., zero magnetic field) and the coefficients of the hyperbolic tangent and hyperbolic cotangent terms in Eqs. (44) and (45) are zero. For the remaining sums, we note that

$$\begin{aligned}
\sum_{q_z(\text{odd})} \frac{1}{\varepsilon_L(\mathbf{q},\omega)} \frac{1}{[(\omega/v)^2-q_z^2]^2} &= -\left[\frac{\partial}{\partial y} \sum_{q_z(\text{odd})} \frac{1}{\varepsilon_L(\mathbf{q},\omega)} \frac{1}{y-q_z^2} \right]_{y=(\omega/v)^2} \\
&= \tilde{C}(\omega) \left[\frac{L}{4\Gamma} \tanh\left[\frac{\Gamma L}{2}\right] \frac{\Gamma^2-q_\parallel^2}{[\Gamma^2+(\omega/v)^2]^2} \right. \\
&\quad + \frac{L}{8(\omega/v)^3} \frac{1}{[\Gamma^2+(\omega/v)^2]^2} \tan\left[\frac{\omega L}{2v}\right] \\
&\quad \times \left\{ \left[q_\parallel^2 + \left[\frac{\omega}{v}\right]^2 \right] \left[\Gamma^2 + \left[\frac{\omega}{v}\right]^2 \right] + 2\left[\frac{\omega}{v}\right]^2 (q_\parallel^2-\Gamma^2) \right\} \\
&\quad \left. - \left[\frac{Lv}{4\omega}\right]^2 \frac{q_\parallel^2+(\omega/v)^2}{\Gamma^2+(\omega/v)^2} \sec^2\left[\frac{\omega L}{2v}\right] \right],
\end{aligned} \tag{48}$$

$$\begin{aligned}
\sum_{q_z(\text{even})} \frac{\eta_{q_z}}{\varepsilon_L(\mathbf{q},\omega)} \frac{1}{[(\omega/v)^2-q_z^2]^2} &= -\left[\frac{\partial}{\partial y} \sum_{q_z(\text{even})} \frac{\eta_{q_z}}{\varepsilon_L(\mathbf{q},\omega)} \frac{1}{y-q_z^2} \right]_{y=(\omega/v)^2} \\
&= \tilde{C}(\omega) \left[\frac{L}{4\Gamma} \coth\left[\frac{\Gamma L}{2}\right] \frac{\Gamma^2-q_\parallel^2}{[\Gamma^2+(\omega/v)^2]^2} \right. \\
&\quad - \frac{L}{8(\omega/v)^3} \frac{1}{[\Gamma^2+(\omega/v)^2]^2} \cot\left[\frac{\omega L}{2v}\right] \\
&\quad \times \left\{ \left[q_\parallel^2 + \left[\frac{\omega}{v}\right]^2 \right] \left[\Gamma^2 + \left[\frac{\omega}{v}\right]^2 \right] + 2\left[\frac{\omega}{v}\right]^2 (q_\parallel^2-\Gamma^2) \right\} \\
&\quad \left. - \left[\frac{Lv}{4\omega}\right]^2 \frac{q_\parallel^2+(\omega/v)^2}{\Gamma^2+(\omega/v)^2} \csc^2\left[\frac{\omega L}{2v}\right] \right].
\end{aligned} \tag{49}$$

The substitution of these results into Eqs. (22) and (23) determines the probability function of the high-velocity energy loss for a fast charged particle penetrating across a finite plasma slab, with proper accounting of phonon polarization and magnetic field jointly corresponding to the excitation of bulk and surface magnetopolaritons for finite slab size L. In null magnetic field, we find considerable simplification of the formulation. After a lengthy and tedious calculation, we obtain from Eq. (23), for $\omega_c = 0$

$$U=-L\tilde{C}(\omega)-\frac{2q_\parallel}{q_\parallel^2+\omega^2/v^2}\left[\sin\left[\frac{\omega L}{2v}\right]\frac{1}{1+\varepsilon_q^{-1}}+\cos\left[\frac{\omega L}{2v}\right]\frac{1}{1+\bar{\varepsilon}_q^{-1}}\right][\tilde{C}(\omega)-1]^2\,, \tag{50}$$

where ε_q and $\bar{\varepsilon}_q$ appearing in Eq. (50) are given by the zero-field limits, obtained from Eqs. (42) and (43) with $\varepsilon_q^{-1}=\tilde{C}(\omega)\tanh(q_\parallel L/v)$, $\bar{\varepsilon}_q=\tilde{C}(\omega)\coth(q_\parallel L/v)$. The first term in Eq. (50) corresponds to L times the probability per unit path length for an infinite crystal (in the absence of a magnetic field). The remaining terms represent the boundary corrections in the limit of large L. We thus write $P(q_\parallel,\omega)$ as the sum of two terms [see Eqs. (26a)]: (i) $LP'_\infty(q_\parallel,\omega)$, with $P'_\infty(q_\parallel,\omega)$ as the probability per unit slab thickness for an infinite medium; and (ii) $P_b(q_\parallel,\omega)$, which arises from boundary effects. Inserting the expressions for ε_q^{-1} and $\bar{\varepsilon}_q$, for $\omega_c=0$, we obtain

$$\begin{aligned}P_b(q_\parallel,\omega)=&\frac{(Ze)^2}{\pi^2\hbar v^2}\frac{q_\parallel}{(q_\parallel^2+\omega^2/v^2)^2}\\&\times\mathrm{Im}\left\{\left[\sin^2\left[\frac{\omega L}{2v}\right]\coth\left[\frac{q_\parallel L}{2}\right]+\cos^2\left[\frac{\omega L}{2v}\right]\tanh\left[\frac{q_\parallel L}{2}\right]\right]\tilde{C}(\omega)\right.\\&-\coth\left[\frac{q_\parallel L}{2}\right]\left[\tanh\left[\frac{q_\parallel L}{2}\right]-1\right]^2\left[\sin^2\left[\frac{\omega L}{2v}\right]\frac{1}{\tilde{C}^{-1}-\tanh(q_\parallel L/2)}\right.\\&\left.\left.+\cos^2\left[\frac{\omega L}{2v}\right]\frac{1}{\tilde{C}^{-1}-\coth(q_\parallel L/2)}\right]\right\}.\end{aligned} \tag{51}$$

The first two terms in Eq. (51) proportional to $\tilde{C}$ give rise to surface energy losses at the *bulk* polariton frequencies, whereas the last two terms correspond to losses at the symmetric and antisymmetric *surface* polariton frequencies. We note that the *bulk* and *surface* terms produce a decrease in loss and an additional loss, respectively [see Eq. (27a)]. Integrating over frequency, weighting $P_b(q_\parallel,\omega)$ with the energy transfer quantum $\hbar\omega$, we obtain the corresponding surface energy loss $W_b(q_\parallel)$ as

$$\begin{aligned}W_b(q_\parallel)=&-\frac{(Ze)^2}{2\pi v^2}\frac{q_\parallel}{(q_\parallel^2+\omega_+^2/v^2)^2}\left[\frac{\omega_p^2+\Omega^2}{\varepsilon_\infty^2}\right]\left[\frac{\omega_+^2-A^2}{\omega_+^2-\omega_-^2}\right]\left[\sin^2\left[\frac{\omega_+ L}{2v}\right]\coth\left[\frac{q_\parallel L}{2}\right]+\cos^2\left[\frac{\omega_+ L}{2v}\right]\tanh\left[\frac{q_\parallel L}{2}\right]\right]\\&+\frac{(Ze)^2}{2\pi v^2}\frac{q_\parallel}{(q_\parallel^2+\omega_{a(+)}^2/v^2)^2}\left[\frac{\omega_p^2+\Omega^2}{\varepsilon_a^2(q_\parallel)}\right]\left[\frac{\omega_{a(+)}^2-A^2}{\omega_{a(+)}^2-\omega_{a(-)}^2}\right]\sin^2\left[\frac{\omega_{a(+)}L}{2v}\right]\coth\left[\frac{q_\parallel L}{2}\right]\left[1-\tanh\left[\frac{q_\parallel L}{2}\right]\right]^2\\&+\frac{(Ze)^2}{2\pi v^2}\frac{q_\parallel}{(q_\parallel^2+\omega_{s(+)}^2/v^2)^2}\left[\frac{\omega_p^2+\Omega^2}{\varepsilon_s^2(q_\parallel)}\right]\left[\frac{\omega_{s(+)}^2-A^2}{\omega_{s(+)}^2-\omega_{s(-)}^2}\right]\cos^2\left[\frac{\omega_{s(+)}L}{2v}\right]\coth\left[\frac{q_\parallel L}{2}\right]\left[1-\tanh\left[\frac{q_\parallel L}{2}\right]\right]^2,\end{aligned} \tag{52}$$

where $A^2\equiv\omega_p^2\omega_{\mathrm{TO}}^2/(\omega_p^2+\Omega^2)$,

$$\varepsilon_a(q_\parallel)\equiv\varepsilon_\infty+\tanh\left[\frac{q_\parallel L}{2}\right],\quad \varepsilon_s(q_\parallel)\equiv\varepsilon_\infty+\coth\left[\frac{q_\parallel L}{2}\right], \tag{53}$$

$$\omega_\pm^2\equiv\omega_{\mathrm{TO}}^2+\frac{\omega_p^2}{\varepsilon_\infty}+\frac{\Omega^2}{\varepsilon_\infty}\pm\left[\left[\omega_{\mathrm{TO}}^2+\frac{\omega_p^2}{\varepsilon_\infty}+\frac{\Omega^2}{\varepsilon_\infty}\right]^2-4\frac{\omega_p^2\omega_{\mathrm{TO}}^2}{\varepsilon_\infty}\right]^{1/2} \tag{54}$$

and $\omega_{s(\pm)}$, $\omega_{a(\pm)}$ are obtained from $\omega_\pm$ in Eq. (54) by replacing ε_∞ by $\varepsilon_s(q_\parallel)$, $\varepsilon_a(q_\parallel)$, respectively. Integrating over $q_\parallel$, our calculation yields the surface energy loss W_b as the sum of the two terms, W_{b1} and W_{b2}, with

$$\begin{aligned}W_{b1}=&-\frac{(Ze)^2}{v^2\varepsilon_\infty^2}(\omega_p^2+\Omega^2)\left[\frac{\omega_+^2-A^2}{\omega_+^2-\omega_-^2}\right]\left[\sin^2\left[\frac{\omega_+ L}{2v}\right]\int_0^\infty dq_\parallel\left[\frac{q_\parallel}{q_\parallel^2+\omega_+^2/v^2}\right]^2\coth\left[\frac{q_\parallel L}{2}\right]\right.\\&\left.+\cos^2\left[\frac{\omega_+ L}{2v}\right]\int_0^\infty dq_\parallel\left[\frac{q_\parallel}{q_\parallel^2+\omega_+^2/v^2}\right]^2\tanh\left[\frac{q_\parallel L}{2}\right]\right]\end{aligned} \tag{55}$$

and

$$W_{b2}=\frac{(Ze)^2}{v^2}(\omega_p^2+\Omega^2)\int_0^\infty dq_\parallel\, q_\parallel^2\left[\frac{\omega_{a(+)}^2(q_\parallel)-A^2}{\omega_{a(+)}^2(q_\parallel)-\omega_{a(-)}^2(q_\parallel)}\right]\sin^2\left[\frac{\omega_{a(+)}(q_\parallel)L}{2v}\right]\times\frac{\coth(q_\parallel L/2)}{\varepsilon_a^2(q_\parallel)}\left[\frac{1-\tanh(q_\parallel L/2)}{q_\parallel^2+\omega_{a(+)}^2(q_\parallel)/v^2}\right]^2$$
$$+\frac{(Ze)^2}{v^2}(\omega_p^2+\Omega^2)\int_0^\infty dq_\parallel\, q_\parallel^2\left[\frac{\omega_{s(+)}^2(q_\parallel)-A^2}{\omega_{s(+)}^2(q_\parallel)-\omega_{s(-)}^2(q_\parallel)}\right]\cos^2\left[\frac{\omega_{s(+)}(q_\parallel)L}{2v}\right]\times\frac{\coth(q_\parallel L/2)}{\varepsilon_s^2(q_\parallel)}\left[\frac{1-\tanh(q_\parallel L/2)}{q_\parallel^2+\omega_{s(+)}^2(q_\parallel)/v^2}\right]^2. \quad (56)$$

It is of interest to examine the dependence of W_{b1}, W_{b2} on the slab thickness L. In the limit of small slab thickness ($t\equiv\omega_p L/v\ll 1$), we obtain an analytic result for W_{b1},

$$W_{b1}=-\frac{(Ze)^2}{v\omega_+\varepsilon_\infty^2}(\omega_p^2+\Omega^2)\left[\frac{\omega_+^2-A^2}{\omega_+^2-\omega_-^2}\right]\times\left\{\frac{1}{t_+}\sin^2\left[\frac{t_+}{2}\right]+\frac{t_+}{2}\cos^2\left[\frac{t_+}{2}\right]\left[\ln\left[\frac{1}{t_+}\right]+\frac{1.57}{t_+}\right]\right\}, \quad (57)$$

where $t_+\equiv\omega_+ L/v$. In Fig. 1 we plot $W_b\equiv W_{b1}+W_{b2}$ and W_{b1}, given by Eqs. (55) and (56), as functions of t. The values of ω_{LO}, ω_{TO}, and ω_p are taken to be 5.50×10^{13}, 5.045×10^{13}, and 3.130×10^{13} sec^{-1}, respectively. The high-frequency dielectric constant is taken to be $\varepsilon_\infty=10.94$ for GaAs so that [see Eq. (40)] $\varepsilon_L(0)=\varepsilon_\infty\omega_{LO}^2/\omega_{TO}^2=13.0$. The W_{b1} term subtracts from the LW'_∞ term for arbitrary slab thickness. Also, as Fig. 1 shows, the W_{b2} term is positive when the slab is sufficiently thin. As the slab thickness increases *both* W_{b1} and W_{b2} approach zero from below. Such behavior was discussed by Ritchie[1] for energy loss to a plasma slab in the absence of electron-phonon coupling.

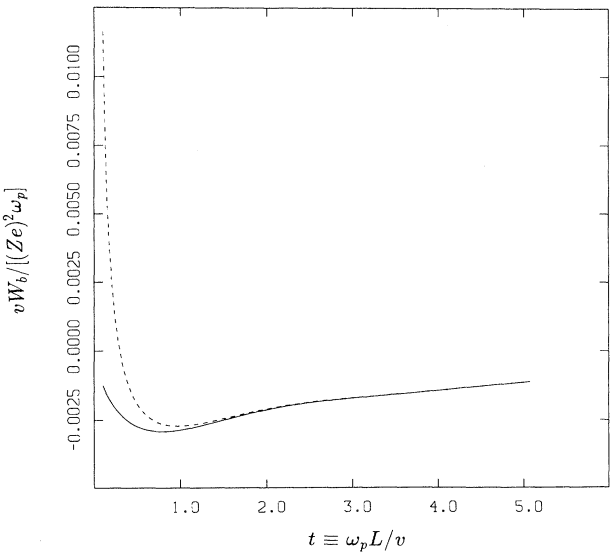

FIG. 1. Calculated energy loss $W_b\equiv W_{b1}+W_{b2}$ (solid curve) and W_{b1} (dashed curve) as a function of the variable $t\equiv\omega_p L/v$. The calculations are based on Eqs. (55) and (56), the high-frequency dielectric constant $\varepsilon_\infty=10.94$ and $\omega_{LO}=1.76\omega_p$, $\omega_{TO}=1.61\omega_p$ for GaAs.

VII. CONCLUSIONS

This work has been directed at the determination of charged particle energy loss in a solid-state plasma film or slab of finite thickness. In particular, we have focused attention on features involving penetration of the slab by the passing particle, and nonlocal dispersive response phenomena of the plasma, as well as well-defined slab-collective-mode excitations. In this, our considerations addressed conditions appropriate to semiconductors, including dynamic phonon polarization phenomena and magnetic field effects in conjunction with plasma response, corresponding to the excitation of bulk and surface magnetopolaritons for a finite slab size.

Our description of plasma response for the dielectric slab was formulated in terms of the RPA inverse dielectric function of the quantum plasma in the diagonal approximation, subject to the boundary condition of specular reflection of electrons at the slab surfaces. In the case of particle motion parallel to the slab surfaces, we discussed the stopping power for motion both inside and outside the slab subject to nonlocal dispersive corrections of the finite slab. For the *inside* case at high velocity, we have found modifications to the results of Núñez, Echenique, and Ritchie due to the finite width of the slab.

We have also examined the total work done by a charged particle penetrating across the plasma slab or film, determining the probability function $P(q_\parallel,\omega)$ (for energy transfer $\hbar\omega$ with momentum $\hbar q_\parallel$) within the diagonal approximation of RPA slab plasma response, making contact with Ritchie's early work and also treating the formulation for thin 2D inversion-layer–quantum-

well structures as well. Our incorporation of nonlocal dispersive slab response features was seen to be most prominent at low velocity of the impingent particle.

In orienting this study toward semiconductor microstructures we also incorporated the dynamics of phonon polarization into the response nature of the magnetoplasma slab to determine the role of bulk and surface magnetopolaritons in the energy loss of a high-velocity charged particle penetrating across the finite slab. The magnetic field aspects of our formulation will facilitate further future analysis of this important probe in the context of energy loss. Our detailed field-free calculations have clearly demonstrated energy-loss contributions associated with the excitation of symmetric and antisymmetric slab surface polaritons as well as bulk polaritons, with computations carried out in full for GaAs extending the earlier work of Ritchie to include features appropriate to semiconductors microstructure devices.

ACKNOWLEDGMENTS

One of us (G.G.) was supported in part by a grant from the Natural Sciences and Engineering Research Council of Canada and the University of Lethbridge Research Fund. G.G. would like to thank P. M. Echenique for hospitality at the Universidad del Pais Vasco, San Sebastian, Spain, where some of this work was done.

[1]R. H. Ritchie, Phys. Rev. **106**, 874 (1957).
[2]S. R. Streight and D. L. Mills, Phys. Rev. B **40**, 10 488 (1989).
[3]H. Ibach and D. L. Mills, *Electron Energy Loss Spectroscopy and Surface Vibrations* (Academic, New York, 1982).
[4]G. Eliasson, P. Hawrylak, and J. J. Quinn, Phys. Rev. B **35**, 5569 (1987).
[5]W. L. Schaich, Phys. Rev. B **24**, 686 (1981); Surf. Sci. **122**, 175 (1982).
[6]B. N. J. Persson and J. E. Demuth, Phys. Rev. B **30**, 5968 (1984); B. N. J. Persson, Solid State Commun. **24**, 573 (1977); B. N. J. Persson and S. Andersson, Phys. Rev. B **29**, 4382 (1984).
[7]G. Gumbs, Phys. Rev. B **39**, 5186 (1989).
[8]P. Lambin, J. P. Vigneron, and A. A. Lucas, Phys. Rev. B **32**, 8203 (1985).
[9]J. R. Hayes, A. F. J. Levi, and W. Wiegmann, Phys. Rev. Lett. **54**, 1570 (1985).
[10]A. F. J. Levi, J. R. Hayes, P. M. Platzman, and W. Wiegmann, Phys. Rev. Lett. **55**, 2071 (1985).
[11]S. Bending, C. Zhang, K. von Klitzing, E. Marclay, P. Guéret, and H. P. Meier, Phys. Rev. B **39**, 12 981 (1989).
[12]R. Núñez, P. M. Echenique, and R. H. Ritchie, J. Phys. C **13**, 4229 (1980).
[13]T. L. Ferrell, P. M. Echenique, and R. H. Ritchie, Solid State Commun. **32**, 419 (1979).
[14]R. H. Ritchie and A. L. Marusak, Surf. Sci. **4**, 234 (1966).
[15]F. Garcia Molinar and F. Flores, J. Phys. **38**, 851 (1977).
[16](a) N. J. M. Horing, E. Kamen, and H.-L. Cui, Phys. Rev. B **32**, 2184 (1985); (b) H.-L. Cui, N. J. M. Horing, and G. Gumbs, preceding paper Phys. Rev. B **43**, 2106 (1991).
[17]D. M. Newns, Phys. Rev. B **1**, 3304 (1970).
[18]N. J. M. Horing, H. C. Tso, and G. Gumbs, Phys. Rev. B **36**, 1588 (1987).
[19]N. J. M. Horing and M. M. Yildiz, Ann. Phys. (N.Y.) **97**, 216 (1976).
[20]N. J. M. Horing and M. M. Yildiz, Phys. Lett. **44A**, 386 (1973).